J Mater Sci (2009) 44:2541–2547
DOI 10.1007/s10853-009-3331-0

Preparation and mesostructure control of highly ordered zirconia particles having crystalline walls

Hirobumi Shibata · Tomoaki Morita · Taku Ogura · Keishi Nishio · Hideki Sakai · Masahiko Abe · Mutsuyoshi Matsumoto

Received: 26 November 2008 / Accepted: 9 February 2009 / Published online: 5 March 2009

Abstract Mesostructured zirconia particles having monoclinic-type crystalline walls were prepared using a low-temperature crystallization technique. Crystalline zirconia particles with highly-ordered mesostructures were obtained through the sol–gel process of zirconium sulfate tetrahydrate at 333 K in the presence of molecular self-assemblies of cetyltrimethylammonium bromide (CTAB) or mixtures of CTAB and anionic molecules such as sodium dodecyl sulfate and sodium *p*-toluenesulfonate. Variations in the molar ratios of CTAB and the chemical species of anionic molecules led to the variations in the periods of highly-ordered zirconia having crystalline walls. Calcination of the mesostructured zirconia particles prepared using templates consisting solely of CTAB yielded crystalline mesoporous zirconia particles.

Introduction

Mesoporous materials [1–6] synthesized using molecular self-assemblies of surfactants as templates have highly ordered pore structures with high specific surface area. These materials have gathered increasing attention due to their possible applications to catalysts, adsorbents, and separating materials. To precisely control the pore structures and pore sizes, ionic surfactants having various alkyl chain lengths [7–9] have been used and organic materials have been added to the surfactant aggregates [10, 11]. In particular, molecular self-assemblies of cationic surfactants–anionic surfactants [12–14], cationic surfactants–cationic surfactants [12, 15], and cationic surfactants–nonionic surfactants [16–18] mixed systems have been used as templates to produce mesoporous materials with controlled pore structures and sizes.

The walls of as-fabricated mesoporous materials are generally amorphous. The problem is that the heat treatment of amorphous mesoporous materials to remove the surfactants leads to the crystallization of the walls that result in the collapse of uniform mesopore structures. Various methods have been used to provide mesoporous materials with crystalline walls. Ozin et al. and Yang et al. have prepared mesoporous materials with thick walls using triblock copolymers as templates [19–22]. Inagaki et al. have synthesized organic-silica hybrid particles using organic–inorganic hybrid materials as silica sources [23, 24]. Domen et al. [25] have reported the calcination method for introducing crystal structures to the walls without the collapse of the ordered pore structures using amorphous mesoporous material with carbon in their pores as starting material. Liu et al. [26] have described the replica method using mesoporous SBA-15 silica as template material. Although the methods using inorganic templates are one of the promising techniques for the crystallization of walls of highly-ordered mesostructures, complicated processes to remove inorganic templates are required. We have recently succeeded in the synthesis of mesoporous titania particles having anatase-type

H. Shibata (✉) · T. Morita · K. Nishio · M. Matsumoto
Faculty of Industrial Science and Technology, Tokyo University of Science, 2641 Yamazaki, Noda, Chiba 278-8510, Japan
e-mail: shibata@rs.noda.tus.ac.jp

T. Ogura · H. Sakai · M. Abe
Faculty of Science and Technology, Tokyo University of Science, 2641 Yamazaki, Noda, Chiba 278-8510, Japan

H. Sakai · M. Abe · M. Matsumoto
Institute of Colloid and Interface Science, Tokyo University of Science, 1-3 Kagurazaka, Shinjuku-ku, Tokyo 162-8601, Japan

nanocrystalline thin walls through a simple route using a low-temperature crystallization technique in the presence of a typical cationic surfactant for the preparation of mesoporous materials [27, 28].

Zirconia has been used as catalyst support due to its chemical stability against acid and base. Sulfated zirconia produced by treating zirconia with sulfuric acid works as a strong solid acid and is expected to be used as an acid catalyst for the synthesis of chemical products as a substitute for liquid acid catalysts [29–31]. Increasing the surface area is very important for the improvement of catalytic properties, because catalytic reactions occur at the surfaces of solid catalysts. Mesoporous materials with walls consisting of zirconia will be efficient solid acid catalysts. In addition, crystallization of the wall of mesoporous zirconia will endow the material with high thermal stability.

This study aims at synthesis of mesoporous zirconia particles having crystalline wall using the low-temperature crystallization technique we developed in the presence of cationic surfactants. Furthermore, the effect of adding anionic molecules on the structural properties of zirconia particles was investigated.

Experimental section

Zirconium sulfate tetrahydrate (Kanto Chemical Co., Inc.) and cetyltrimethylammonium bromide (Aldrich; CTAB) were used as zirconia precursor and template material, respectively. Sodium dodecyl sulfate (Wako Pure Chemical Industries, Ltd.; SDS) and sodium *p*-toluenesulfonate (Wako Pure Chemical Industries, Ltd.; ST) were used as anionic molecules that were added to the template material.

The total concentration of the surfactant solution composed of CTAB and anionic molecules was fixed at 60 mM. The molar ratio of CTAB:anionic molecules was changed from 10:0 to 0:10. A total of 60 mM surfactant solution and 720 mM zirconium sulfate aqueous solution were mixed at room temperature and stirred at 333 K for 24 h. Then, the obtained particles were filtrated, washed with pure water, and dried at 393 K for 10 h. When the molar ratio of CTAB:anionic molecules was changed from 5:5 to 0:10, no zirconia particles were obtained. Therefore, the characterization of zirconia particles were performed only for the samples synthesized at CTAB:anionic molecules = 10:0 to 6:4. Structural properties of the prepared zirconia particles were investigated using X-ray diffraction (XRD) measurements (Philips, X'pert-MPD CuKα radiation), transmission electron microscope (TEM; Hitachi model H-7650: W filament) and high-resonance TEM (HRTEM; Hitachi model H-9500: LaB6 filament) observations. TEM and HRTEM were operated at accelerating voltages of 120 and 300 kV, respectively. Nitrogen adsorption–desorption isotherm measurements were carried out using a Quantachrome Autosorb-1-MP. Adsorbed and desorbed amounts of nitrogen were calculated by measuring the pressure of nitrogen 10 min after the dosage and degas, respectively.

Results

We investigated first whether the template consisting of cationic surfactant is effective in the preparation of mesostructured zirconia as in the preparation of mesostructured titania. Figure 1 shows the XRD patterns of the obtained zirconia particles. The molar ratio of CTAB:anionic molecules was 10:0. The low-angle XRD pattern (Fig. 1a) shows three diffraction peaks at 2.23, 3.79, and 4.43° due to the (100), (110), and (200) reflections, respectively, indicating the formation of highly ordered hexagonal structures. The distance between the centers of the nearest pores calculated using Bragg's equation on the basis of the (100) reflection is about 4 nm. This distance almost coincides with that of mesoporous titania having hexagonal structures [25, 26]. Figure 1b shows a wide-angle XRD pattern of the obtained zirconia particles. This pattern exhibits peaks ($2\theta = 27$, 45 and 59°) assigned to monoclinic-type zirconia, suggesting that the walls of the

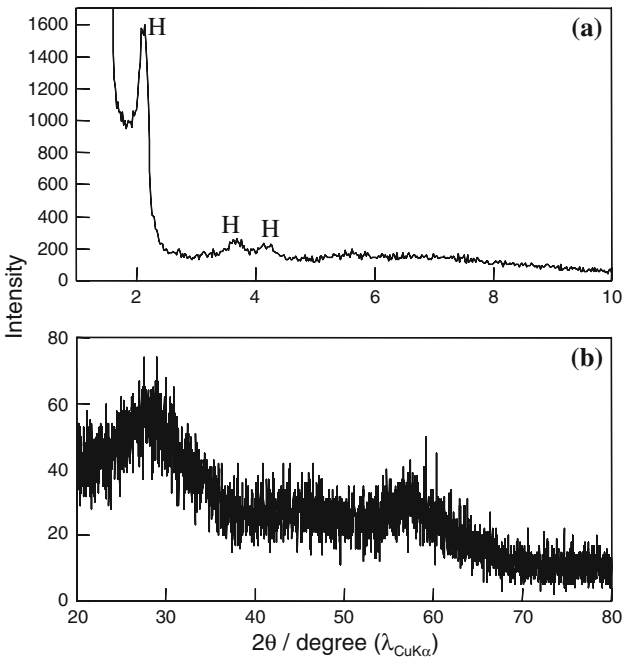

Fig. 1 **a** Low- and **b** wide-angle XRD patterns of zirconia-CTAB composite particles. "H" denotes the peaks assignable to hexagonal mesostructure

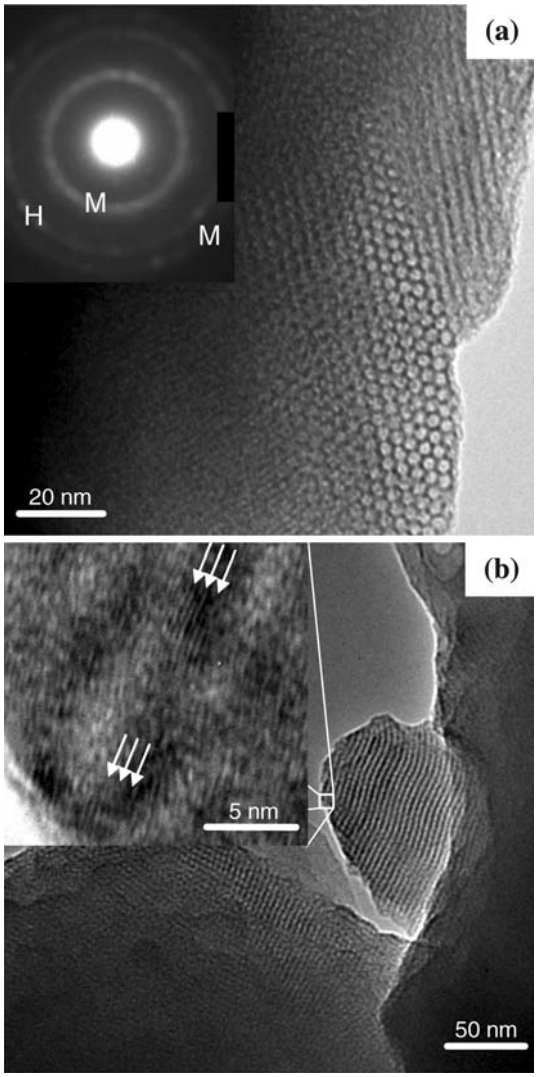

Fig. 2 Transmission electron microscopy (**a**) and high resolution transmission electron microscopy (**b**) images of zirconia-CTAB composite particles. M and H in the electron diffraction pattern (inset of (**a**)) represent Debye rings assigned to monoclinic- and hexagonal-type zirconia, respectively

mesostructured zirconia particles are monoclinic-type zirconia.

Figure 2a shows a typical TEM image and an electron diffraction (ED) pattern (inset) of the mesostructured zirconia. The TEM image shows that zirconia particles have highly ordered honey-comb structures. The period of the hexagonal mesostructure in the zirconia particles estimated from the TEM image coincides with the value of about 4 nm calculated from the low-angle XRD pattern. The ED pattern shows Debye rings assigned to monoclinic- and hexagonal-type crystal structures of zirconia. The high resolution TEM image shown as an inset of Fig. 2b clearly reveals lattice fringes in the wall of mesostructured particles. The fringes with a spacing of 0.26 nm are consistent with the spacing of (020) crystallographic plane of monoclinic zirconia. These results indicate that the walls of the mesostructured particles synthesized by stirring at 333 K in the presence of CTAB have crystalline zirconia frameworks.

Next, we investigated the effect of adding SDS on the structural properties of crystalline mesostructured zirconia-surfactants composite particles. Figure 3 shows the XRD patterns of zirconia-surfactants composite particles synthesized by using CTAB/SDS mixed template systems. Peaks at around $2\theta = 2.2$, 3.8, and 4.4° assigned to hexagonal mesostructures are present in the low-angle XRD patterns of the composite particles prepared at CTAB:SDS = 10:0 and 9:1. In contrast, the low-angle XRD patterns of particles synthesized at CTAB:SDS = 7:3 and 6:4 show diffraction peaks around 2.1 and 4.2° assignable to lamellar mesopore structures. Table 1 lists the molar ratios of CTAB:SDS, 2θ and d_{100} values calculated on the basis of the diffraction peaks due to the (100) plane of hexagonal or lamellar mesostructures using Bragg's equation. The values of 2θ decrease and the d_{100} values increase with increasing molar ratio of SDS in both hexagonal and lamellar mesostructure regions. The values at CTAB:SDS = 9:1 and 8:2 are almost the same. These results suggest that the interplanar spacing in the mesostructures can be controlled by changing the molar ratio in the CTAB/SDS mixed template system. All the wide-angle XRD patterns exhibit peaks assigned to monoclinic-type zirconia crystal (Fig. 3b). These results indicate that CTAB/SDS mixed template systems can give crystalline zirconia particles with hexagonal and lamellar mesostructures, the interplanar spacing of which can be controlled with the variations in the molar ratio of SDS.

Figure 4 shows XRD patterns of zirconia particles prepared using CTAB/ST mixed template systems. The molar ratios of CTAB:ST are changed from 10:0 to 6:4. The low-angle XRD patterns (Fig. 4a) show three diffraction peaks assigned to hexagonal mesostructures. This indicates that CTAB/ST mixed template systems are also effective in synthesizing hexagonal-type mesostructured zirconia particles irrespective of the amount of ST used in this study. Table 2 lists the molar ratios of CTAB:ST, 2θ and d_{100} values (interplanar spacing) calculated on the basis of the positions of the diffraction peaks due to the (100) plane of hexagonal mesostructures using Bragg's equation. The value of 2θ decreases and the d_{100} value increases with increasing molar ratio of ST. The size of templates of CTAB/ST mixed systems varies with the molar ratio of ST as that of CTAB/SDS mixed systems. The peaks assigned to monoclinic-type crystal structure are present in all the wide-angle XRD patterns (Fig. 4b). These results indicate that the mesostructured zirconia particles with crystalline walls can be also prepared using CTAB/ST mixed template systems.

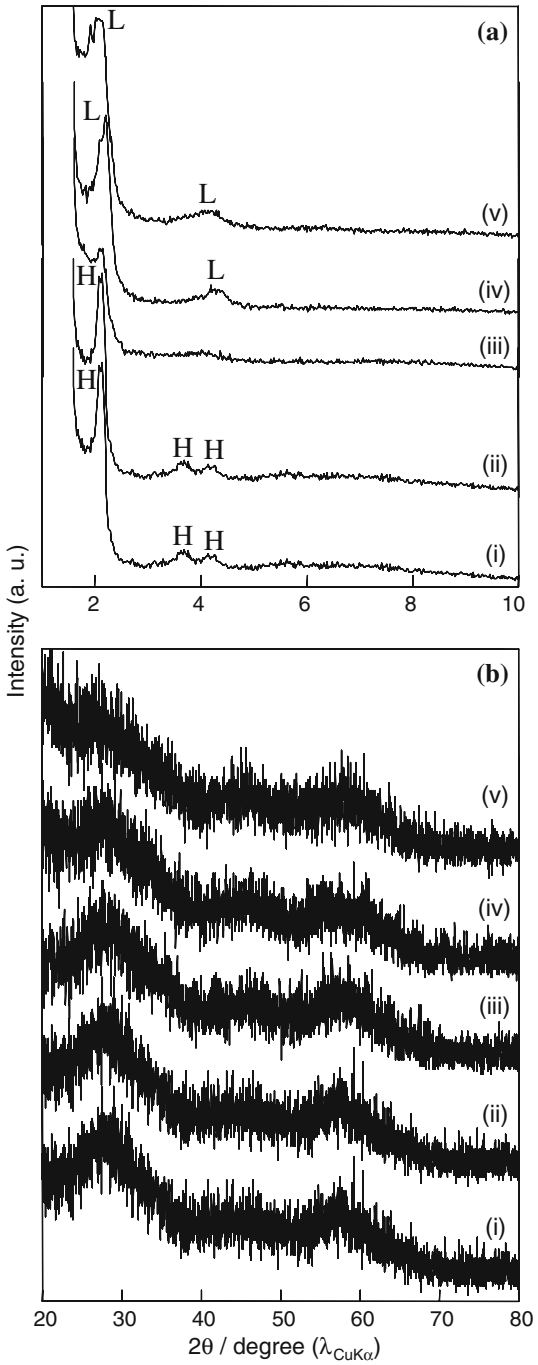

Fig. 3 **a** Low- and **b** wide-angle XRD patterns of zirconia particles prepared using CTAB/SDS mixed template systems. The curves (i)–(v) show the diffraction patterns of zirconia fabricated with molar ratios of CTAB:SDS = 10:0, 9:1, 8:2, 7:3 and 6:4, respectively. "H" and "L" denote the peaks assigned to hexagonal and lamellar mesostructures, respectively

Finally, we investigated the effect of calcination on the structural properties of the mesostructured zirconia particles. The zirconia particles prepared with a molar ratio of CTAB:anionic molecules = 10:0 were calcined twice at 723 K for 6 h with heating and cooling rates of 1 K/min.

Table 1 Effect of molar ratio of CTAB to SDS on the d_{100} values of zirconia-surfactant composite particles

Molar ratio (CTAB:SDS)	2θ (°)	d_{100} Value (nm)
10:0	2.23	3.96
9:1	2.07	4.27
8:2	2.09	4.23
7:3	2.19	4.03
6:4	2.09	4.23

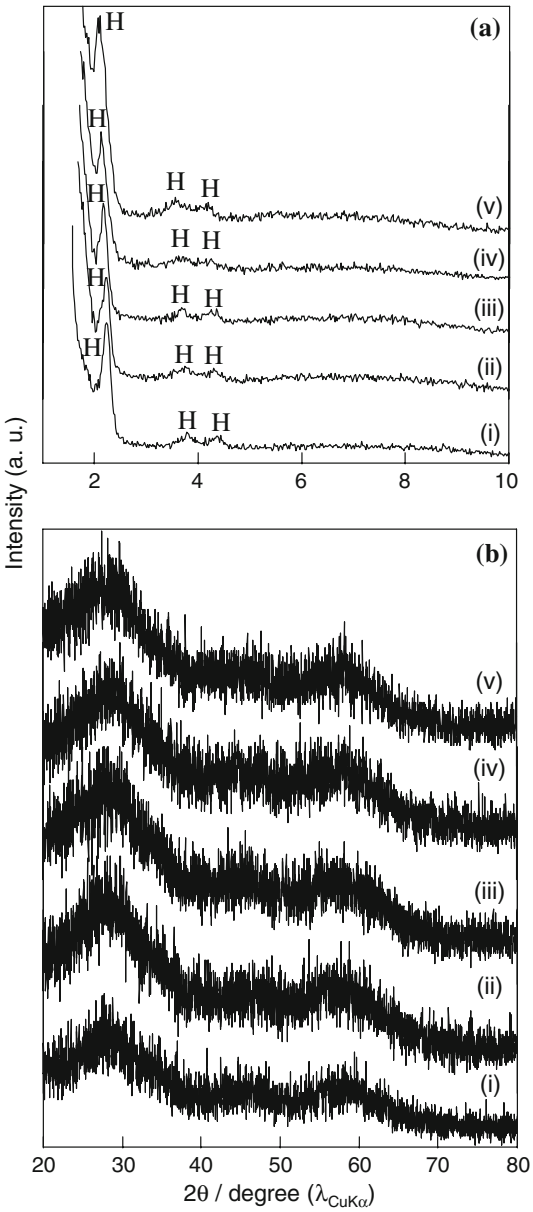

Fig. 4 **a** Low- and **b** wide-angle XRD patterns of zirconia particles prepared using CTAB/ST mixed template systems. The curves (i)–(v) show the diffraction patterns of zirconia fabricated with molar ratios of CTAB:ST = 10:0, 9:1, 8:2, 7:3 and 6:4, respectively. "H" denote the peak assigned to hexagonal mesostructure

Table 2 Effect of molar ratio of CTAB to ST on the d_{100} values of zirconia-surfactant composite particles

Molar ratio (CTAB:ST)	2θ (°)	d_{100} Value (nm)
10:0	2.23	3.96
9:1	2.21	4.00
8:2	2.17	4.07
7:3	2.13	4.15
6:4	2.09	4.23

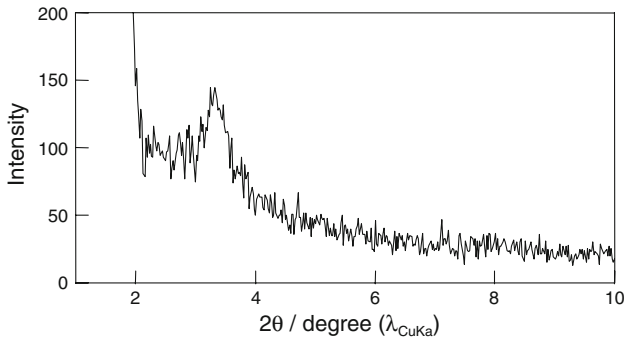

Fig. 5 Low-angle XRD pattern of zirconia particles after calcination

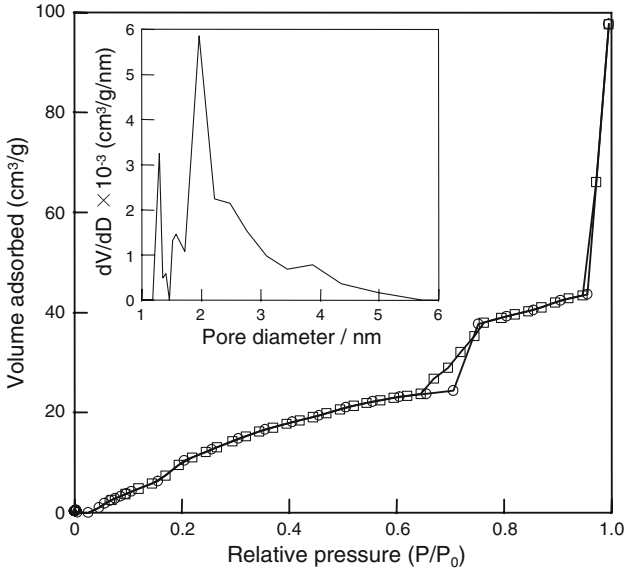

Fig. 7 N_2 adsorption–desorption isotherms and BJH pore size distribution (inset) deduced from adsorption branches of zirconia particles. Circles (○) and squares (□) represent the adsorption and desorption isotherms, respectively

Figure 5 shows the low-angle XRD pattern of the zirconia particles after the calcination. The peak around 3.3° is assignable to the (100) reflection of hexagonal mesostructures. This result suggests that the zirconia particles possess a hexagonally aligned pore structure after the calcination. The distance between the centers of the nearest pores calculated using Bragg's equation on the basis of the (100) reflection is about 3 nm. Figure 6 shows a TEM image of the zirconia particles after the calcination. The TEM image shows a structure with highly-ordered hexagonal arrays of pores of the size of about 2 nm. Nitrogen adsorption and desorption measurements of the particles revealed that the adsorption isotherms exhibit behaviors characteristic of solids with mesopores (type IV) and show a hysteretic phenomenon suggesting the presence of cylindrical pores (Fig. 7). The surface area is 98 m^2/g. BJH pore size distribution deduced from the adsorption branch (Fig. 7, inset) shows the presence of pores with sizes around 2 nm. This pore size value is in good agreement with those calculated from the low-angle XRD pattern and estimated from the TEM image. These results demonstrate the successful preparation of "crystalline" mesoporous zirconia particles with highly-ordered hexagonal pore structures.

The zirconia particles with hexagonal mesostructures prepared by using the mixed templates of CTAB and anionic molecules yielded, after the calcination, XRD patterns and TEM images similar to those prepared with a

Fig. 6 TEM image of zirconia particles after calcination

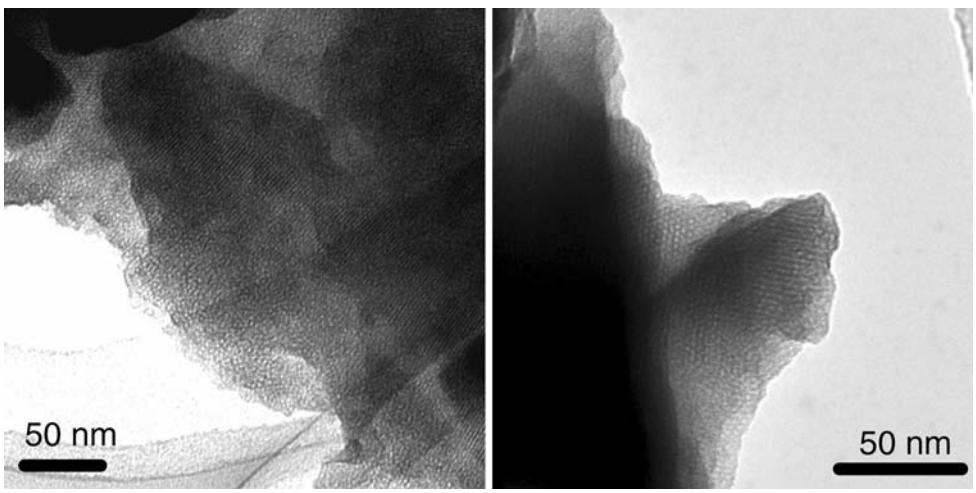

molar ratio of CTAB:anionic molecules = 10:0, suggesting the presence of pores of the size of about 2 nm. However, the measurements of nitrogen adsorption and desorption isotherms of the particles using our instrument encountered with problems: 99 min was not sufficient for the pressure to be equilibrated and the setting of the waiting time longer than 99 min was impossible. The lamellar structures of the zirconia particles collapsed during the calcination judging from the XRD patterns.

Discussion

Variations in the mesostructure and in the period of the mesostructure of the zirconia particles prepared using CTAB/SDS and CTAB/ST mixed templates are explained on the basis of packing parameter. Packing parameter is the volume of a surfactant divided by the product of the cross-section of the hydrophilic moiety and the molecular length. Rod micelles form when the packing parameter is between 1/3 and 1/2. In contrast, lamellae form when the packing parameter is around unity [32]. Mesostructured zirconia with hexagonal structures is fabricated when templates of rod micelles are aligned hexagonally. The results obtained by using CTAB/SDS mixed template systems indicate that the packing parameter increases with an increase in molar ratio of SDS. This gives rise to an increase in the period of the hexagonal mesostructure with increasing molar ratio of SDS. Lamellae form when the molar ratio of SDS increases further. The addition of anionic SDS to cationic CTAB yields the formation of a quasi two-chain type surfactant due to the electrostatic interaction (Fig. 8). Neutralization of the charge of CTAB leads to three effects: (1) suppression of repulsion between the positive charges of CTAB molecules, (2) decrease in the number of hydrated water molecules of CTAB head group, and (3) increase in the solubility of the quasi two-chain type surfactant in the hydrophobic portion of the micelle compared with CTAB. The volume of the hydrophobic moiety of SDS and that of CTAB are not very different from each other and are not affected significantly by the neutralization of the hydrophilic moieties. The packing parameter of the quasi two-chain type surfactant is larger than that of CTAB [33]. This brings about increase in the diameter of the rod micelle and the period of the hexagonal mesostructure with increasing molar ratio of SDS and the subsequent phase transition from hexagonal mesostructures to lamellae.

The results obtained using CTAB/ST mixed template systems indicate that the packing parameter increases with an increase in molar ratio of ST. The addition of ST to CTAB brings about the three effects as in the case of SDS. The difference is that the volume of the hydrophobic moiety of ST is much smaller than that of CTAB. The volume of the hydrophobic moiety of ST contributes only to a small extent to the total volume of the salt of CTAB and ST [33]. The experimental results indicate that the effect of the increase in the cross-section of the hydrophilic moiety due to the addition of ST on the packing parameter is smaller than the total of the three effects due to the neutralization and the increase in the hydrophobic moiety due to the addition of ST.

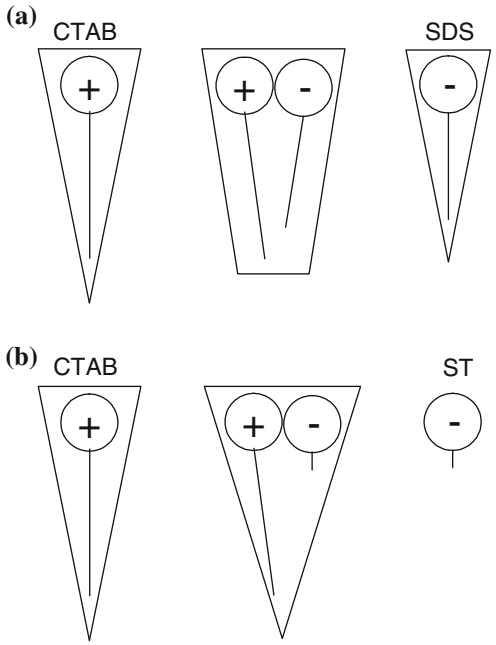

Fig. 8 Schematic illustration of quasi two-chain surfactants formed in the micelles. Parts (**a**) and (**b**) show the salts of CTAB/SDS and CTAB/ST, respectively

Conclusion

In this study, we have prepared highly ordered crystalline zirconia particles with hexagonal and lamellar mesostructures. Crystalline zirconia particles with hexagonal mesostructures have been successfully prepared using CTAB or CTAB/anionic molecules mixed template systems at a temperature as low as 333 K. We have investigated the effect of the addition of anionic molecules on the mesostructures of the crystalline mesostructured zirconia. The type of mesostructure and the period of the mesotructure of zirconia are controlled with the variations in the species of anionic molecules and the molar ratio of CTAB/anionic molecules. To the best of our knowledge, this is the first report on the control of the type and the period of mesostructured materials with crystalline walls. Further, calcination of the mesostructured zirconia particles prepared using templates consisting solely of CTAB yielded crystalline mesoporous zirconia particles. The present

methodology will find applications to catalysts and separation materials, because the type and the period of mesostructured materials can be controlled easily without using complicated processes.

References

1. Kresge CT, Leonowicz ME, Roth WJ, Vartuli JC, Beck JS (1992) Nature 359:710
2. Attard GS, Glyde JC, Goltner CG (1995) Nature 378:366
3. Davis SA, Burkett SL, Mendelson NH, Mann S (1997) Nature 385:420
4. Huo Q, Leon R, Petroff PM, Stucky GD (1995) Science 268:1324
5. Ogawa M, Kikuchi T (1998) Adv Mater 14:1077
6. Zhang Y, Weidenkaff A, Reller A (2002) Mater Lett 54:375
7. Huo Q, Margolese DI, Stucky GD (1996) Chem Mater 8:1147
8. Ogawa M (1994) J Am Chem Soc 116:7941
9. Ogawa M (1997) Langmuir 13:1853
10. Lebeau B, Fowler CE, Hall SR, Mann S (1999) J Mater Chem 9:2279
11. Sayari A, Yang Y, Kruk M, Jeroniec M (1999) J Phys Chem B 103:3651
12. Lind A, Spliethoff B, Lindèn M (2003) Chem Mater 15:813
13. Pevzner S, Regev O, Lind A, Lindèn M (2003) J Am Chem Soc 125:652
14. Chen F, Song F, Li Q (1999) Microporous Mesoporous Mater 29:305
15. Khushalani D, Kuperman N, Coombs N, Ozin GA (1996) Chem Mater 8:2188
16. Dai LR, Wang TW, Bu LT, Chen G (2001) Colloids Surf A 181:151
17. Ryoo R, Joo SH, Kim JM (1999) J Phys Chem B 103:7435
18. Qi L, Ma J, Cheng H, Zhao Z (1998) Chem Mater 10:1623
19. Haseloh S, Choi SY, Mamak M, Coombs N, Petrov S, Chopra N, Ozin GA (2004) Chem Commun 1460
20. Choi SY, Mamak M, Coombs N, Chopra N, Ozin GA (2004) Adv Funct Mater 14:335
21. Choi SY, Mamak M, Speakman S, Chopra N, Ozin GA (2005) Small 1:226
22. Yang P, Zhao D, Margolese DI, Chmelka BF, Stucky GD (1998) Nature 396:152
23. Kapoor MP, Inagaki S, Ikeda S, Kakiuchi K, Suda M, Shimada T (2005) J Am Chem Soc 127:8174
24. Kapoor MP, Yang Q, Inagaki S (2004) Chem Mater 16:1209
25. Katou T, Lee B, Lu D, Kondo JN, Hara M, Domen K (2003) Angew Chem 115:2484
26. Liu B, Baker RT (2008) J Mater Chem 18:5200
27. Shibata H, Ogura T, Mukai T, Ohkubo T, Sakai H, Abe M (2005) J Am Chem Soc 127:16396
28. Shibata H, Mihara H, Mukai T, Ogura T, Kohno H, Ohkubo T, Sakai H, Abe M (2006) Chem Mater 18:2256
29. Babou F, Coudurier G, Vedrine JC (1995) J Catal 152:341
30. Tatsumi T, Matsuhashi H, Arata K (1996) Bull Chem Soc Jpn 69:1191
31. Sun Y, Ma S, Du Y, Yuan L, Wang S, Yang J, Deng F, Xiao F-S (2005) J Phys Chem B 109:2567
32. Butt H-J, Graf K, Kappl M (2006) Physics and chemistry of interface. Wiley, Weinheim
33. Salkar RA, Mukesh D, Samant SD, Manohar C (1998) Langmuir 14:3778